

Quantum chemical studies on the molecular structure, spectroscopic and electronic properties of (6-Methoxy-2-oxo-2H-chromen-4-yl)-methyl pyrrolidine-1-carbodithioate

MERYEM EVEGEN, HASAN TANAK*

Department of Physics, Faculty of Arts and Sciences, Amasya University, 05000, Amasya, Turkey

In this paper, the molecular geometry, vibrational frequencies and chemical shifts of (6-Methoxy-2-oxo-2H-chromen-4-yl)methyl pyrrolidine-1-carbodithioate in the ground state have been calculated using the Hartree-Fock and density functional methods with the 6-311++G(d,p) basis set. To investigate the nonlinear optical properties of the title compound, the polarizability and the first hyperpolarizability were calculated. The conformational properties of the molecule have been determined by analyzing molecular energy properties. Using the time dependent density functional theory, electronic absorption spectra have been calculated. Frontier molecular orbitals, natural bond orbitals, natural atomic charges and thermodynamical parameters were also investigated by using the density functional theory calculations.

Keywords: *coumarin; vibrational spectroscopy; density functional theory; chemical shifts; electronic properties*

© Wrocław University of Technology.

1. Introduction

Coumarins are wide spread in nature, like flavonoids, which are also extensively represented in plants, and whose beneficial properties have only recently gained recognition [1]. They are structurally closely related to chromenes and show various biological activities [2–6]. Some coumarin derivatives, due to their outstanding optical properties, have also found a place and subsequent use in laser dyes, non-linear optical chromophores, fluorescent whiteners, fluorescent probes and solar energy collectors [7–10]. Because of its unique medicinal properties, structural variability, low cost and low toxicity, the coumarin scaffold has been broadly used in the design and development of a number of pharmaceutically important compounds [11]. Depending on the nature as well as pattern of the substitution, coumarins may display a variety of pharmacological, biochemical and therapeutic properties [12, 13].

By means of increasing development of computational chemistry in the past decade, the research of theoretical modeling of drug design, functional material design, etc., has become much more mature than ever. Many important chemical and physical properties of biological and chemical systems can be predicted from the first principles by various computational techniques [14]. In recent years, density functional theory (DFT) has been a shooting star in theoretical modeling. The development of better and better exchange-correlation functionals made it possible to calculate many molecular properties with comparable accuracies to traditional correlated ab-initio methods, at more favorable computational costs [15]. Literature survey revealed that the DFT has a great accuracy in reproducing the experimental values of geometry, vibrational frequency, electronic absorption spectra, etc. [16, 17].

In the previous publication, the X-ray crystallography and IR spectra of (6-Methoxy-2-oxo-2H-chromen-4-yl)-methyl pyrrolidine-1-carbodithioate were studied [18]. In spite of its

*E-mail: hasantanak@gmail.com

importance, mentioned above, no theoretical calculation concerning (6-Methoxy-2-oxo-2H-chromen-4-yl)-methyl pyrrolidine-1-carbodithioate has been published yet. The aim of this study is to investigate the spectral and structural properties of the coumarin compound, (6-Methoxy-2-oxo-2H-chromen-4-yl)-methyl pyrrolidine-1-carbodithioate, using the Hartree-Fock (HF) and density functional theory (DFT) calculations. In this work, the molecular structure, vibrational spectra and assignments, ^1H - and ^{13}C NMR spectra, electronic absorption spectra, frontier molecular orbitals (FMO), natural bond orbitals (NBO), natural atomic charges, nonlinear optical properties and thermodynamical parameters of (6-Methoxy-2-oxo-2H-chromen-4-yl)-methyl pyrrolidine-1-carbodithioate were investigated. These calculations are valuable for providing insight into molecular properties of coumarins.

2. Theoretical methods

The molecular geometry was taken directly from the X-ray diffraction experimental result without any constraints. The HF and DFT calculations of the compound have been done using the Gaussian 09W software [19]. The vibrational frequencies were calculated at the HF and DFT/B3LYP levels for the optimized structures and the predicted frequencies were scaled by 0.96 for DFT/B3LYP and 0.89 for HF. Vibrational band assignments were made using the Gauss-View 5 software [20]. Besides, the thermodynamic functions of the title compound at different temperatures were calculated on the basis of vibrational analysis, using B3LYP/6-311++G(d,p) level. To identify the conformational flexibility, two selected degrees of torsional freedom, T(S1-C18-N6-C19) and T(S1-C17-C14-C15), were changed from -180° to $+180^\circ$ in steps of 10° , and the molecular energy profiles were obtained at the DFT/B3LYP level. The ^1H - and ^{13}C -NMR chemical shifts were calculated using the Gauge-Independent Atomic Orbital (GIAO) approach [21] applying B3LYP and HF methods with 6-311++G(d,p) basis set. The geometry of the compound, together with that of tetramethylsilane (TMS), was fully optimized.

The obtained ^1H - and ^{13}C -NMR chemical shifts were derived from the equation $\delta = \Sigma_0 - \Sigma$, where δ is the chemical shift, Σ is the absolute shielding and Σ_0 is the absolute shielding of the standard (TMS) [22]. The solvent effect on the theoretical ^1H - and ^{13}C -NMR parameters was included using the the integral equation formalism polarizable continuum model (IEF-PCM) [23] provided by Gaussian 09W. Ethanol and dimethylsulfoxide (DMSO) were used as solvents. The linear polarizability and first hyperpolarizability properties of the title compound were predicted by molecular polarizabilities basing on theoretical calculations. In addition, NBO and FMOs were performed at the B3LYP/6-311++G(d,p) level.

3. Results and discussion

3.1. Optimized geometries

The atomic numbering scheme for the title crystal [18] and the theoretical geometric structure of the title compound are shown in Fig. 1. The crystal structure of the title compound is triclinic and space group is P-1. The crystal structure parameters are $a = 6.7223$ (2) Å, $b = 8.0369$ (2) Å, $c = 15.4101$ (5) Å, $\alpha = 75.320$ (2)°, $\beta = 88.482$ (1)°, $\gamma = 78.842$ (1)° and $V = 789.93$ (4) Å³ [18].

The optimized bond lengths, bond angles and torsion angles of the title compound have been obtained using the HF and DFT/B3LYP methods with the 6-311++G(d,p) basis set. Theoretical and experimental geometric parameters are listed in Table 1. When the X-ray structure of the title compound is compared with its optimized counterparts (Fig. 2), slight conformational discrepancies are observed between them. The title crystal is not planar. The dihedral angle between the 2H-chromene (O4/C8-C16) ring and pyrrolidine (N6/C18-C22) ring is 75.24 (16)° for X-ray [18], whereas the dihedral angle has been calculated as 67.65° for B3LYP and 70.00° for HF. The orientation of the both the rings is defined by the torsion angles C22-N6-C18-S1 (178.00°), N6-C18-S1-C17 (-170.98°), C18-S1-C17-C14 (103.72°) and S1-C17-C14-C15 (-99.35°) which have been calculated as 178.48° , -176.56° , 105.99° and -104.04° for B3LYP, and 178.56° , -174.45° ,

98.78° and -107.40° for HF, respectively. In the title compound, the bond lengths and angles are within normal ranges and they are comparable with those of related compounds [24–26].

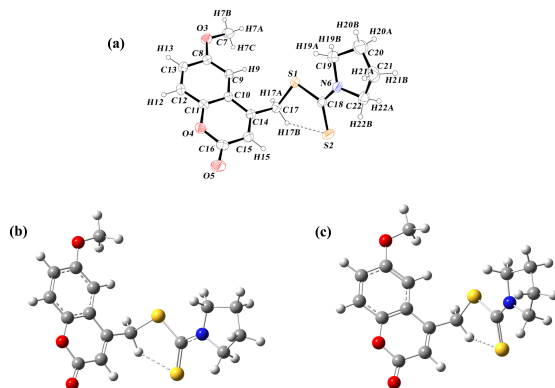


Fig. 1. (a) The experimental geometric structure of the title compound [18], (b) DFT optimized structure of the title compound, (c) HF optimized structure of the title compound.

It is well known that DFT-optimized bond lengths are usually longer and more accurate than HF due to the inclusion of electron correlation [27]. On the other hand, according to calculated results, the HF method correlates better for the bond distance compared with the DFT/B3LYP method (Table 1). The maximum difference of bond lengths between the experimental and the predicted values has been found at C20–C21 bond with the difference being 0.061 Å for B3LYP method, and with a value 0.053 Å for HF method. The root mean square error (RMSE) is obtained as 0.018 Å for HF and 0.021 Å for B3LYP, indicating that the bond lengths predicted by the HF method show a good correlation with the experimental values. For bond angles, the opposite trend was observed. As can be seen from Table 1, both the biggest difference and the RMSE for the bond angles calculated by the B3LYP method are smaller than those predicted by HF. A global comparing of the structures obtained by the theoretical calculations has been done by superimposing the molecular skeleton with that obtained from X-ray diffraction [28], giving a RMSE of 0.247 Å for B3LYP and 0.324 Å for HF method (Fig. 2). As a result, the B3LYP calculation

well reproduces the the 3-D geometry of the title compound.

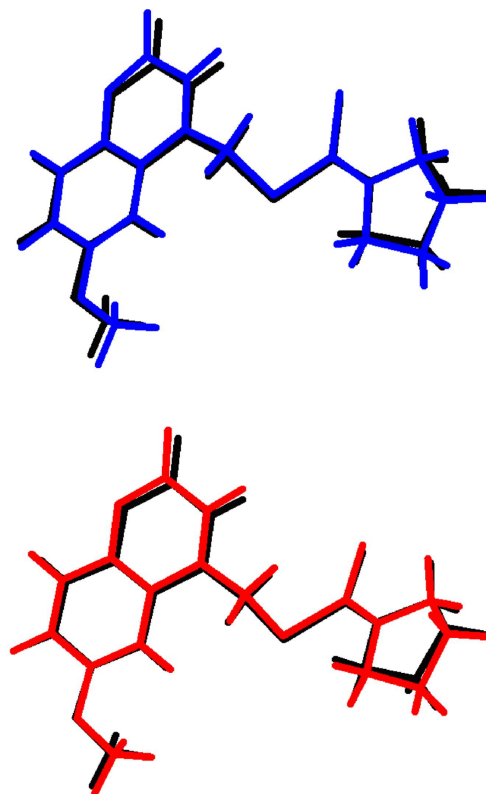


Fig. 2. Superimposition of the calculated HF (top) and DFT (bottom) and experimental structures of (6-Methoxy-2-oxo-2H-chromen-4-yl)-methyl pyrrolidine-1-carbodithioate.

3.2. Conformational analysis

In order to define the preferential position of pyrrolidine and chrome rings, a preliminary search of low energy structures was performed using B3LYP/6-311++G(d,p) computations as a function of the selected degrees of torsional freedom T(S1–C18–N6–C19) and T(S1–C17–C14–C15). The respective values of the selected degrees of torsional freedom, T(S1–C18–N6–C19) and T(S1–C17–C14–C15), are -0.81° and -99.34° in X-ray structure [18], whereas the corresponding values in DFT optimized geometry are -1.35° and -104.04°. Molecular energy profiles with respect to rotations about the selected torsion angles are presented in Fig. 3.

Table 1. Selected molecular structure parameters.

Parameters	Experimental [18]	Calculated 6-311++G(d,p)	
		B3LYP	HF
Bond lengths [Å]			
S1–C18	1.787 (2)	1.815	1.785
S1–C17	1.813 (2)	1.839	1.823
S2–C18	1.666 (2)	1.669	1.669
O3–C8	1.358 (3)	1.364	1.347
O3–C7	1.403 (3)	1.421	1.398
O4–C16	1.364 (3)	1.390	1.344
O4–C11	1.375 (3)	1.365	1.353
O5–C16	1.199 (3)	1.204	1.180
N6–C18	1.313 (3)	1.341	1.320
N6–C19	1.465 (3)	1.479	1.472
N6–C22	1.480 (3)	1.478	1.472
C8–C9	1.386 (3)	1.388	1.374
C8–C13	1.391 (3)	1.406	1.399
C9–C10	1.395 (3)	1.411	1.405
C10–C11	1.395 (3)	1.400	1.377
C10–C14	1.445 (3)	1.411	1.405
C11–C12	1.385 (3)	1.396	1.390
C12–C13	1.361 (3)	1.380	1.369
C14–C15	1.341 (3)	1.355	1.332
C14–C17	1.502 (3)	1.504	1.507
C15–C16	1.446 (4)	1.455	1.466
C19–C20	1.507 (4)	1.532	1.526
C20–C21	1.474 (5)	1.535	1.527
C21–C22	1.505 (5)	1.531	1.525
Max. difference ^a		0.061	0.053
RMSE		0.021	0.018
Bond angles [°]			
C18–S1–C17	102.70 (11)	103.03	105.31
C8–O3–C7	118.4 (2)	118.57	119.95
C16–O4–C11	121.98 (18)	122.35	123.06
C18–N6–C19	126.0 (2)	126.05	126.07
C18–N6–C22	123.3 (2)	122.29	122.30
C19–N6–C22	110.6 (2)	111.64	111.61
O3–C8–C9	124.1 (2)	124.75	124.86
O3–C8–C13	115.9 (2)	115.39	115.54
C9–C8–C13	119.9 (2)	119.85	119.59
C8–C9–C10	120.1 (2)	120.49	120.54

Table 1. (Continuation) Selected molecular structure parameters.

Parameters	Experimental [18]	Calculated 6-311++G(d,p)	
		B3LYP	HF
C11–C10–C9	118.4 (2)	118.48	118.70
C11–C10–C14	117.6 (2)	117.46	117.19
C9–C10–C14	123.99 (19)	124.04	124.09
O4–C11–C12	116.88 (19)	116.76	116.65
O4–C11–C10	121.7 (2)	122.19	122.29
C12–C11–C10	121.4 (2)	121.03	121.04
C13–C12–C11	119.3 (2)	119.76	119.71
C12–C13–C8	120.9 (2)	120.35	120.38
C15–C14–C10	119.0 (2)	119.10	118.80
C15–C14–C17	121.1 (2)	119.94	120.25
C10–C14–C17	119.93 (19)	120.94	120.92
C14–C15–C16	123.0 (2)	122.99	122.28
O5–C16–O4	116.9 (2)	117.99	119.15
O5–C16–C15	126.6 (3)	126.11	124.49
O4–C16–C15	116.5 (2)	115.88	116.35
C14–C17–S1	110.94 (16)	112.80	113.25
N6–C18–S2	124.10 (18)	123.67	123.54
N6–C18–S1	111.67 (17)	111.57	112.58
S2–C18–S1	124.21 (15)	124.75	123.86
N6–C19–C20	104.6 (2)	103.67	103.58
C21–C20–C19	105.7 (3)	103.34	103.21
C20–C21–C22	105.6 (3)	103.57	103.41
N6–C22–C21	103.7 (2)	103.75	103.61
Max. Difference ^a		2.36	2.61
RMSE		0.831	1.168
Torsion angles [°]			
C22–N6–C18–S1	178.00	178.48	178.56
N6–C18–S1–C17	–170.98	–176.56	–174.45
C18–S1–C17–C14	103.72	105.99	98.78
S1–C17–C14–C15	–99.35	–104.04	–107.40

^aMaximum differences between the bond lengths and angles computed using theoretical methods and those obtained from X-ray diffraction

As can be seen from the Fig. 3, the low energy domains for T(S1–C18–N6–C19) are located at 0° and 180°, while they are located at –100° and 120° for T(S1–C17–C14–C15). Energy difference between the most favorable and unfavorable conformers, which arises from rotational potential barrier calculated with respect to the two selected

torsion angles, is 0.036 Hartree for T(S1–C18–N6–C19) and 0.14 Hartree for T(S1–C17–C14–C15), when both selected degrees of torsional freedom are considered. It must be remarked that the selected torsion angles in the crystal structure of the title compound are close to the value in the global energy minimum.

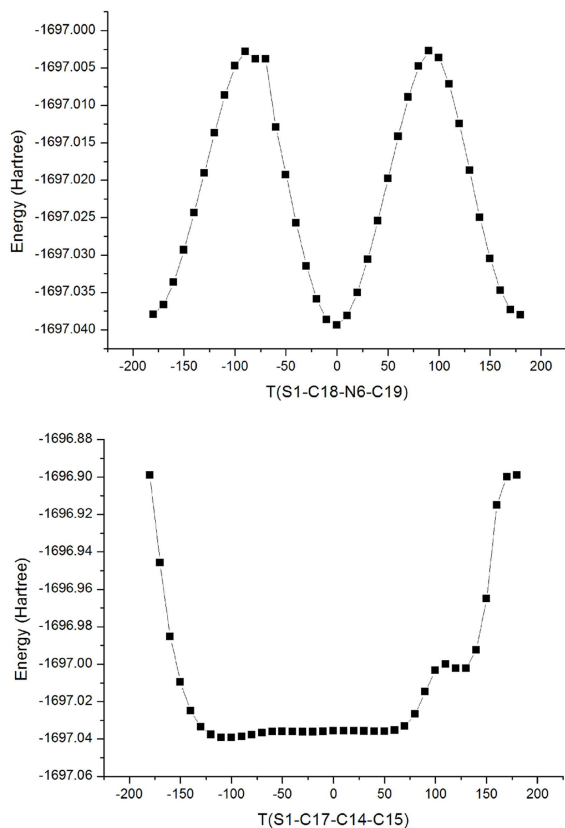


Fig. 3. Potential energy profile using the DFT/B3LYP method for the internal rotation around the C18–N6 and C17–C14 bonds.

3.3. Vibrational analysis

In this study, harmonic vibrational frequencies were calculated using the DFT/B3LYP and HF methods with the 6-311++G(d,p) basis set. Using the Gauss-View molecular visualisation program, the vibrational band assignments were made. In order to facilitate assignment of the observed peaks, the vibrational frequencies have been analyzed and the calculation for the title compound have been compared with the experimental results. The vibrational frequencies in the region 4000 cm^{-1} to 600 cm^{-1} are given in Table 2. The IR spectra contain some characteristic bands of the stretching vibrations of the C–H, C–H₂, C–H₃, C=O, C–O, C–N, C=S and C–S groups.

3.3.1. C–H vibrations

C–H is known as characteristic vibrational frequency. In the literature, the in-plane and out-of-plane bending vibrational frequencies are obtained within their characteristic region. The aromatic compounds commonly exhibit C–H stretching vibrations in the region of 3150 cm^{-1} to 2900 cm^{-1} [29, 30] which is the characteristic region for the ready identification of C–H stretching vibrations in plane. In this region the bands are not appreciably affected by the nature of the substituents. In our present work, C–H aromatic stretching are of medium intensity and in the expected region, lie within the range of 3089 cm^{-1} to 3078 cm^{-1} by B3LYP and 3019 cm^{-1} to 2998 cm^{-1} by HF. Also C–H in-plane and out-of-plane bending vibrations were observed in the range of 1300 cm^{-1} to 1000 cm^{-1} and 900 cm^{-1} to 675 cm^{-1} [31], respectively. In the title compound, C–H aromatic rocking bands have been found at 1348 cm^{-1} , 1184 cm^{-1} and 1092 cm^{-1} by B3LYP and at 1344 cm^{-1} , 1205 cm^{-1} and 1076 cm^{-1} by HF method. Besides, C–H aromatic wagging bands are only out-of-plane bending vibrations which is observed at 871 cm^{-1} , 816 cm^{-1} and 728 cm^{-1} by B3LYP and 887 cm^{-1} , 832 cm^{-1} and 731 cm^{-1} by HF. Rahman et al. [32] has found the wagging type vibrations of the C–H bonds at 820 cm^{-1} and 794 cm^{-1} theoretically, which correlates nicely with an experimental peak at 800 cm^{-1} .

3.3.2. Methyl group vibrations

The title molecule possesses one C–H₃ group. The C–H methyl group stretching vibrations are highly localized and generally observed in the range of 3000 cm^{-1} to 2900 cm^{-1} [31, 33]. In 7-Methoxy-4-methylcoumarin, the bands observed at 3001 cm^{-1} , 2964 cm^{-1} , 2951 cm^{-1} in FT-IR spectrum and the bands observed at 3000 cm^{-1} and 2951 cm^{-1} in Raman spectrum were assigned to CH₃ asymmetric stretching vibrations [34]. The CH₃ symmetric stretching vibrations were observed at 2902 cm^{-1} and 2855 cm^{-1} in the FT-IR spectrum [34]. In this study, the peaks calculated at 3011 cm^{-1} and 2938 cm^{-1} for B3LYP and 2924 cm^{-1} and 2866 cm^{-1} for HF are assigned to asymmetric stretching of the methyl group.

The symmetric one is calculated at 2883 cm^{-1} and 2813 cm^{-1} for B3LYP and HF levels, respectively. CH_3 scissoring vibration is also identified at 1460 cm^{-1} for B3LYP, while wagging vibrations are identified at 1444 cm^{-1} , 1184 cm^{-1} , 1158 cm^{-1} and 1120 cm^{-1} and 1450 cm^{-1} , 1205 cm^{-1} , 1181 cm^{-1} and 1045 cm^{-1} for B3LYP and HF, respectively. The calculated wavenumbers of CH_3 group vibrations show the good correlation with the data presented in the literature [35–37].

3.3.3. Methylene vibrations

The asymmetric CH_2 stretching vibrations are generally observed above 3000 cm^{-1} , while the symmetric stretch appears between 3000 cm^{-1} and 2900 cm^{-1} [38]. The CH_2 asymmetric stretching vibration was calculated at 2985 cm^{-1} for B3LYP and at 2889 cm^{-1} for HF, while the symmetric stretching vibrations were predicted at 2926 cm^{-1} and 2924 cm^{-1} for B3LYP and at 2887 cm^{-1} and 2883 cm^{-1} for HF. Similar vibrational modes were also observed for free pyrrolidine [39] or cyclopentene [40] and other pyrrolidine derivatives [41]. The CH_2 two wagging and two twisting out-of-plane deformation vibrations were calculated at 1319 cm^{-1} and 1184 cm^{-1} for B3LYP and at 1335 cm^{-1} and 1205 cm^{-1} for HF and at 1158 cm^{-1} and 1128 cm^{-1} for B3LYP and at 1181 cm^{-1} for HF, respectively. The band at 910 cm^{-1} was assigned to CH_2 rocking in-plane deformation vibration [42]. In the present work, the same vibrations were calculated at 900 cm^{-1} by B3LYP and at 935 cm^{-1} by HF.

3.3.4. C=O and C–O vibrations

Coumarin derivative compounds have two characteristic absorption bands arising from C=O and C–O stretching vibrations. The C=O stretching frequency appears strongly in the IR spectrum in the range of 1600 cm^{-1} to 1850 cm^{-1} because of the large change in dipole moment. The carbonyl group vibrations give rise to characteristic bands in vibration spectra and the characteristic frequency used to study a wide range of compounds. The intensity of these bands can increase owing to conjugation or formation of hydrogen bonds [43]. Moghaddam et al. [44]

assigned C=O stretching absorption in the region of 1744 cm^{-1} to 1717 cm^{-1} for 3-benzyl-2H-pyrano[3,2-chromene-2,5(6H)-dione. In 4-hydroxy-1-thiocoumarin, the C=O stretching was found to be present at 1701 cm^{-1} [43]. In the present study, chromene (C=O) bond stretching vibration was observed at 1708 cm^{-1} experimentally [18], while it has been calculated at 1722 cm^{-1} for B3LYP and at 1767 cm^{-1} for HF. The experimental C–O stretching bands were observed at 1036 cm^{-1} and 1279 cm^{-1} , and were calculated at 900 cm^{-1} to 1214 cm^{-1} for B3LYP and at 935 cm^{-1} to 1233 cm^{-1} for HF. These values are in good agreement with the similar compounds [45, 46].

3.3.5. C–N vibrations

The calculation of C–N stretching frequency is a rather hard job since there are problems in identifying these frequencies from other vibrations [47]. Silverstein et al. [31] identified the C–N stretching absorption in the region of 1382 cm^{-1} to 1266 cm^{-1} for aromatic amines. Tecklenburg et al. [48] located the C–N symmetric stretch in the region of 1120 cm^{-1} to 1150 cm^{-1} . The C–N stretchings were also found to be present at 1248 cm^{-1} and 1199 cm^{-1} by Pajazk et al. [49]. In this study, the C–N stretching vibrations were calculated at 1389 cm^{-1} , 1128 cm^{-1} and 835 cm^{-1} by B3LYP and at 1389 cm^{-1} , 1181 cm^{-1} and 843 cm^{-1} by HF.

3.3.6. C–C vibrations

The aromatic stretching vibrations are very prominent, as they involve double C=C bond in conjugation with the ring. The ring C=C and C–C stretching vibrations are expected within the region of 1620 cm^{-1} to 1390 cm^{-1} [50]. The C=C stretching vibrations of the title compound with very strong intensity are predicted at 1594 cm^{-1} , 1581 cm^{-1} , 1536 cm^{-1} and 1460 cm^{-1} for B3LYP level and at 1604 cm^{-1} , 1566 cm^{-1} and 1475 cm^{-1} for HF level. These olefinic C=C stretching vibrations are also in good agreement with the experimental (at 1590 cm^{-1} , 1558 cm^{-1} , 1544 cm^{-1} and 1482 cm^{-1}) and theoretical (1588 cm^{-1} , 1583 cm^{-1} , 1541 cm^{-1} and 1508 cm^{-1}) values [51]. The stretching vibrational bands for

C–C bond were calculated at 1348 cm^{-1} and 1319 cm^{-1} for B3LYP and at 1344 cm^{-1} and 1335 cm^{-1} for HF.

3.3.7. C=S and C–S vibrations

According to Silverstein et al. [52], the spectra of the compounds in which C=S group is attached to an N atom show absorption bands in the broad region of 1563 cm^{-1} to 700 cm^{-1} . In nitrogen containing thiocarbonyl compounds, the assignment of the C=S stretching frequency has been controversial [53–55]. Mani et al. [56] have reported an absorption band in phenylisothiocyanate near 988 cm^{-1} . The absorption bands in the region of 1180 cm^{-1} to 1150 cm^{-1} have been assigned to the C=S stretching vibrations in thiohydroxamic acids [57]. In this study, the C=S stretching vibration, calculated at 974 cm^{-1} for B3LYP and at 972 cm^{-1} for HF. The C–S group is less polar than carbonyl links and has a considerably weaker band. In consequence, the bond is not intense, and it falls at lower frequencies [58]. Tanak et al. [59] assigned this mode at 680 cm^{-1} and 497 cm^{-1} in FT-IR spectrum. The C–S stretching mode was observed at 672 cm^{-1} for trifluoperazine [60]. In our title molecule the C–S stretching is observed at 660 cm^{-1} in FT-IR spectrum [18]. This band is found to be 666 cm^{-1} and 801 cm^{-1} for HF, and 674 cm^{-1} and 792 cm^{-1} for B3LYP.

3.4. Proton and carbon-13 NMR chemical shift analyses

GIAO ^1H and ^{13}C chemical shift values were calculated using B3LYP and HF methods with the 6-311++G(d,p) basis set in gas phase and the calculated results are given in Table 3. To investigate the solvent effect on the chemical shift values of the compound, based on B3LYP and HF method and IEF-PCM model, two solvents ($\epsilon = 46.7$, DMSO; $\epsilon = 24.55$, ethanol) were selected and the calculated values were also listed in Table 3. Relative chemical shifts were estimated by using the TMS shielding calculated in advance at the same theoretical level as the reference. Calculated ^1H isotropic chemical shielding for TMS at the HF(gas), B3LYP(gas), HF(ethanol), B3LYP(ethanol), HF(DMSO) and B3LYP(DMSO)

are 32.44 ppm, 31.97 ppm, 32.43 ppm, 31.96 ppm, 32.43 ppm and 31.96 ppm, respectively. Also, calculated ^{13}C isotropic chemical shielding for TMS at the HF (gas), B3LYP (gas), HF (ethanol), B3LYP (ethanol), HF (DMSO) and B3LYP (DMSO) are 196.11 ppm, 184.06 ppm, 196.58 ppm, 184.54 ppm, 196.59 ppm and 184.66 ppm, respectively.

We have calculated ^1H chemical shift values (with respect to TMS) of 1.89 ppm to 7.37 ppm at the B3LYP (gas) and 1.73 ppm to 7.81 ppm at HF (gas) level. Besides, they were calculated to be 2.00 ppm to 7.48 ppm at the B3LYP (ethanol), 1.71 ppm to 7.80 ppm at the HF (ethanol), 2.00 ppm to 7.49 ppm at the B3LYP (DMSO) and 1.71 ppm to 7.80 ppm at the HF (DMSO). In (S)-2-Oxopyrrolidin-1-yl Butanamide [61], CH_2 protons of the pyrrolidine ring are observed in the region of 2.47 ppm to 4.50 ppm. In our study, CH_2 protons of the pyrrolidine ring are found in the region of 1.89 ppm to 4.30 ppm at all the B3LYP levels and 1.73 ppm to 3.88 ppm at all the HF levels. In the 3-(1-((methoxycarbonyl)oxy)imino)ethyl)-2H-chromen-2-one, the chemical shift values of chromene ring protons were observed at 7.28 ppm to 8.08 ppm experimentally, and at 7.05 ppm to 7.91 ppm for the HF/6-311++G(d,p) level and 7.26 ppm to 8.41 ppm for the B3LYP/6-311++G(d,p) level [62]. In the present work, the chromene ring protons have been calculated at 6.80 ppm to 7.87 ppm for B3LYP and at 6.73 ppm to 7.81 ppm for HF levels in gas and solution phase.

The ^{13}C NMR chemical shift values (with respect to TMS) have been calculated to be 28.69 ppm to 205.44 ppm for B3LYP (gas), 24.57 ppm to 226.88 ppm for HF (gas), 29.23 ppm to 206.75 ppm for B3LYP (ethanol), 25.04 ppm to 227.35 ppm for HF (ethanol), 29.35 ppm to 206.97 ppm for B3LYP (DMSO) and 25.05 ppm to 227.36 ppm for HF (DMSO). The chromene ring carbons give peaks at 100 ppm to 200 ppm for all methods. These peaks have been observed at 113 ppm to 177 ppm in 7-Acetoxy-4-(bromomethyl)coumarin [63]. As seen from Table 3, ^1H and ^{13}C NMR spectra were a little affected by the change in polarity of the solvent.

Table 2. Comparison of the experimental and calculated vibrational frequencies [cm^{-1}].

Assignments ^a	Experimental [18]	Scaled frequencies with 6-311++G(d,p)	
		B3LYP	HF
ν (C–H) ring	–	3089	3019
ν (C–H) ring	–	3083	3015
ν (C–H) ring	–	3078	2998
ν (C–H ₃) as	–	3011	2924
ν (C–H ₂) as	–	2985	2889
ν (C–H ₂) s	–	2926	2887
ν (C–H ₃) as	–	2938	2866
ν (C–H ₂) s	–	2924	2883
ν (C–H ₃) s	–	2883	2813
ν (C=O)	1708	1722	1767
ν (C=C)	–	1594	1604
ν (C=C) ring	–	1581	1566
ν (C=C) ring	–	1536	1475
ν (C=C) + α (C–H ₃)	–	1460	–
ω (C–H ₃)	–	1444	1450
ν (C–N)	–	1389	1389
ν (C–C) + γ (C–H) ring	–	1348	1344
ν (C–C) + ω (C–H ₂)	–	1319	1335
γ (C–H) ring	–	1246	1251
ν (C–O) ring + ν (C–O) methoxy	1279	1214	1233
γ (C–H) ring + ω (C–H ₂) + ω (C–H ₃)	–	1184	1205
δ (C–H ₂) + ω (C–H ₃)	–	1158	1181
ν (C–N) + δ (C–H ₂)	–	1128	1181
ω (C–H ₃)	–	1120	1045
γ (C–H) ring	–	1109	1045
γ (C–H) ring + ν (C–O) ring	–	1092	1076
ν (C–O) methoxy	1036	1024	1045
ν (C=S)	–	974	972
ν (C–O) ring + γ (C–H ₂)	–	900	935
ω (C–H) ring	–	871	887
ν (C–N)	842	835	843
ω (C–H) ring	–	816	832
ν (C–S) + β (C–H ₂)	–	792	801
ω (C–H) ring	–	728	731
ν (C–S)	660	674	666

^a: ν – stretching; δ – twisting; γ – rocking; ω , wagging; α , scissoring; β , bending; s, symmetric; as – asymmetric

^1H and ^{13}C chemical shift results of the title compound in gas phase are generally closer to the solvent phase. The calculated ^1H and ^{13}C chemical shift values of the title compound are in a good agreement with those of related chromene and pyrrolidine derivatives [64, 65].

Table 3. Theoretical and experimental ^1H and ^{13}C isotropic chemical shifts (with respect to TMS values in ppm) for the title compound.

Atom	Gas		Ethanol		DMSO	
	B3LYP	HF	B3LYP	HF	B3LYP	HF
H7A	3.75	3.67	3.92	3.65	3.93	3.63
H7B	4.14	4.04	4.24	4.03	4.24	4.03
H7C	3.69	3.64	3.88	3.62	3.89	3.65
H9	6.71	7.03	7.06	7.00	7.07	7.02
H12	7.37	7.81	7.48	7.80	7.49	7.80
H13	7.30	7.75	7.48	7.73	7.49	7.74
H15	6.80	6.73	6.77	6.73	6.77	6.72
H17A	4.00	4.03	4.33	3.99	4.35	4.01
H17B	5.50	5.24	5.46	5.23	5.45	5.23
H19A	3.40	3.08	3.47	3.06	3.47	3.06
H19B	3.76	3.46	3.82	3.44	3.82	3.45
H20A	1.98	1.87	2.11	1.85	2.12	1.86
H20B	2.07	1.94	2.13	1.93	2.13	1.93
H21A	1.89	1.73	2.00	1.71	2.00	1.71
H21B	1.95	1.92	2.08	1.91	2.08	1.91
H22A	3.75	3.39	3.77	3.38	3.77	3.38
H22B	4.30	3.88	4.24	3.88	4.18	3.87
C7	56.76	50.26	57.92	50.70	58.08	50.73
C8	163.38	159.94	164.94	160.39	165.10	160.41
C9	106.50	109.31	109.16	109.62	109.44	109.74
C10	126.16	122.12	126.87	122.58	127.00	122.60
C11	158.96	151.76	158.40	152.26	158.49	152.25
C12	124.72	127.27	124.96	127.81	125.04	127.77
C13	127.92	130.96	129.74	131.39	129.90	131.43
C14	159.64	164.12	164.81	164.28	165.16	164.50
C15	122.61	119.57	120.63	120.23	120.64	120.11
C16	163.72	164.98	167.21	165.29	167.44	165.41
C17	42.95	33.34	43.17	33.80	43.29	33.82
C18	205.44	226.88	206.75	227.35	206.97	227.36
C19	53.29	47.80	55.25	48.20	55.44	48.26
C20	30.86	26.30	31.46	26.76	31.59	26.78
C21	28.69	24.57	29.23	25.04	29.35	25.05
C22	60.29	53.03	62.20	53.45	62.38	53.50

3.5. Natural bond orbital analysis

NBO analysis provides an efficient method for studying intra and intermolecular hydrogen bonding and interaction among bonds, and provides a convenient basis for investigating charge transfer or conjugative interaction in molecular systems. The energy of hyperconjugative interactions or the stabilization energy gives the interaction between donor groups and acceptor ones [66, 67]. More intensive interactions between electron donors and electron acceptors depend on larger $E^{(2)}$ value, i.e., the more donating tendency from electron donors to electron acceptors the greater the extent of conjugation of the whole system [68]. For each donor NBO (i) and acceptor NBO (j), the stabilization energy $E^{(2)}$ is estimated by the following equation [69, 70]:

$$E^{(2)} = -q_i \frac{(F_{ij})^2}{\epsilon_j - \epsilon_i} \quad (1)$$

where q_i is the donor orbital occupancy, ϵ_i , ϵ_j are diagonal elements (orbital energies) and F_{ij} is the off-diagonal NBO Fock matrix element. In order to investigate the intramolecular interaction, the stabilization energies of the title compound were performed using the second-order perturbation theory. The results of second-order perturbation theory analysis of the Fock Matrix at B3LYP/6-311++G(d,p) level of theory are collected in Table 4. For the table, the stabilization energies larger than 13 kJ/mol have been chosen.

The NBO analysis has revealed that the intramolecular interactions which are formed by the orbital overlap between bonding (C–S), (C–O), (C–N), (C–C) and (C–H) anti-bonding orbital, result in intramolecular charge transfer causing stabilization of the compound. These interactions are observed as an increase in electron density (ED) in (C–S), (C–C) and (C–O) anti-bonding orbitals that weakens the respective bonds. The electron density of the five conjugated single bonds of pyrrolidine ring (~ 1.98 e) clearly demonstrates strong delocalization. Additionally, the ED of conjugated bond of 2H-chromene ring (~ 1.91 e) clearly shows strong delocalization inside the compound [59].

In the studied compound, strong intramolecular hyperconjugative interactions of π -electrons with the greater energy contributions from C8–C9 \rightarrow C10–C11 (73.94 kJ/mol), C12–C13 (69.93 kJ/mol); C10–C11 \rightarrow C8–C9 (74.48 kJ/mol), C12–C13 (71.68 kJ/mol); C14–C15 (42.21 kJ/mol); C12–C13 \rightarrow C8–C9 (80.67 kJ/mol), C10–C11 (75.53 kJ/mol); C14–C15 \rightarrow O5–C16 (91.54 kJ/mol), C10–C11 (43.76 kJ/mol) are observed for the chromene part of the compound. The hyperconjugative interactions of the $\sigma \rightarrow \sigma^*$ and $\sigma \rightarrow \pi^*$ transitions occur also from various bonds in the compound, such as the hyperconjugative interaction of the σ (C22–H22B) distribute to σ^* (C22–H22B); (C15–H15); (C10–C14); (C14–C17) and (C22–H22A) leading to stabilization of 33.27 kJ/mol, 46.94 kJ/mol, 61.61 kJ/mol, 118.16 kJ/mol and 269.02 kJ/mol, respectively. This enhanced bond further conjugate with antibonding orbital of π^* (C14–C15), which results in strong delocalization of 52.54 kJ/mol.

There is a very weak intramolecular C–H...S hydrogen bond exposed in the NBO analysis results shown in Table 4 caused by the interactions between the sulfur lone-pair LP(2) S2 and the antibonding orbital σ^* (C17–H17B). The lone pair of N6 donates its electrons to the π -type antibonding orbital for (S2–C18). This interaction gives the strongest stabilization to the system of the title compound by 357.01 kJ/mol. In addition, the π^* (C8–C9) NBO conjugates with respective bonds of π^* (C10–C11) and π^* (C12–C13) resulting in an enormous stabilization of 532.95 kJ/mol and 830.56 kJ/mol, respectively.

3.6. Atomic charge analysis

In order to investigate the electron population of each atom of the title compound, the natural population analysis (NPA) atomic charges of the compound were calculated using the DFT/B3LYP method with the 6-311++G(d,p) basis set. The obtained results are given in Table 5. NPA charge plot has been shown in Fig. 4. The NPA analysis shows that the carbon atoms attached to hydrogen atoms are negative, whereas the carbon atoms (C8, C11,

C16) adjacent to the oxygen atoms of the chromene ring are positively charged. The oxygen atoms of chromene fragment and N6 atom of pyrrolidine ring have more negative atomic charges whereas all the hydrogen atoms have positive charges. The maximum positive atomic charge is obtained for C16 atom of carbonyl group when compared with all other atoms. This is due to the attachment of maximum negatively charged O5 atom.

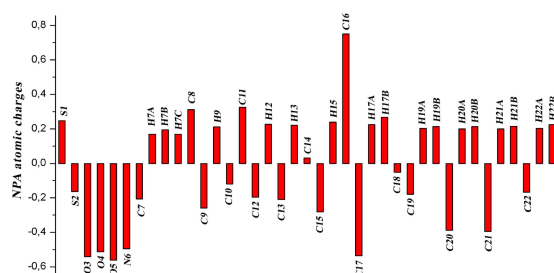


Fig. 4. Natural atomic charges of (6-Methoxy-2-oxo-2H-chromen-4-yl)-methyl pyrrolidine-1-carbodithioate.

3.7. Electronic absorption spectra and frontier molecular orbital analysis

The electronic absorption spectra of the title compound were computed using the TD-DFT method in the gas phase and the DMSO solvent (Fig. 5). The solvent effect was calculated using IEF-PCM method. For TD-DFT calculations, a theoretical absorption band was calculated at 242.43 nm (3.62 eV) with oscillator strength being 0.104. The other absorption peak was calculated at 231.21 nm (5.36 eV) with oscillator strength being 0.114. In addition to the calculations in gas phase, TD-DFT calculations of the title compound in DMSO solvent were performed at 352.01 nm (3.52 eV) with oscillator strength being 0.127 and at 233.41 nm (5.31 eV) with oscillator strength being 0.208. According to the investigations on the frontier molecular orbital (FMO) energy levels of the title compound, we can find that the corresponding electronic transfers happened between the HOMO–1 and LUMO, HOMO–3 and LUMO+1 orbitals, respectively.

Table 4. Selected second-order perturbation energies $E^{(2)}$ associated with $i \rightarrow j$ delocalization in gas phase.

Donor orbital (i)	Type	ED/e	Acceptor orbital (j)	Type	ED/e	$E^{(2)}$ [kJ/mol] ^a	$E(j)-E(i)$ [a.u.] ^b	$F(i,j)$ [a.u.] ^c
S1–C17	σ	1.96731	C14–C15	π^*	0.16017	13.08	0.78	0.046
S1–C18	σ	1.97456	N6–C22	σ^*	0.03367	23.28	0.95	0.065
S2–C18	σ	1.98622	S2–C18	σ^*	0.02661	19.18	0.22	0.033
S2–C18	π	1.98142	N6–C19	σ^*	0.03696	20.06	1.02	0.063
O5–C16	π	1.97927	C14–C15	π^*	0.16017	14.25	0.56	0.040
N6–C19	σ	1.98300	S2–C18	π^*	0.02661	15.92	1.02	0.056
N6–C22	σ	1.98037	S1–C18	σ^*	0.11776	15.29	0.87	0.052
N6–C22	σ	1.98037	C10–C14	σ^*	0.03343	18.01	1.43	0.070
N6–C22	σ	1.98037	C14–C15	π^*	0.16017	14.71	0.91	0.052
N6–C22	σ	1.98037	C14–C17	σ^*	0.02814	31.35	1.60	0.098
N6–C22	σ	1.98037	C15–H15	σ^*	0.01325	16.17	1.32	0.064
N6–C22	σ	1.98037	C22–H22A	σ^*	0.02002	98.68	5.65	0.326
C7–H9	σ	1.99099	O3–C8	σ^*	0.02948	14.50	0.89	0.050
C8–C9	σ	1.97744	C9–C10	σ^*	0.02110	14.96	1.26	0.060
C8–C9	π	1.70329	C10–C11	π^*	0.42279	73.94	0.31	0.069
C8–C9	π	1.70329	C12–C13	π^*	0.29806	69.93	0.31	0.064
C8–C13	σ	1.97225	O3–C7	σ^*	0.00895	13.04	0.99	0.050
C8–C13	σ	1.97225	C8–C9	σ^*	0.02751	17.09	1.27	0.064
C9–H9	σ	1.97491	C8–C13	σ^*	0.02300	16.55	1.09	0.059
C9–H9	σ	1.97491	C10–C11	σ^*	0.03420	16.80	1.09	0.059
C9–C10	σ	1.96573	O3–C8	σ^*	0.02948	17.89	1.05	0.060
C9–C10	σ	1.96573	O4–C11	σ^*	0.03285	15.88	1.04	0.056
C9–C10	σ	1.96573	C8–C9	σ^*	0.02751	14.25	1.26	0.059
C9–C10	σ	1.96573	C10–C11	σ^*	0.03420	15.88	1.25	0.061
C9–C10	σ	1.96573	C10–C14	σ^*	0.03343	13.00	1.40	0.059
C10–C11	σ	1.97068	C9–C10	σ^*	0.02110	15.00	1.25	0.060
C10–C11	σ	1.97068	C11–C12	σ^*	0.02153	18.09	1.25	0.066
C10–C11	π	1.61973	C8–C9	π^*	0.36558	74.48	0.29	0.064
C10–C11	π	1.61973	C12–C13	π^*	0.29806	71.68	0.30	0.066
C10–C11	π	1.61973	C14–C15	π^*	0.16017	42.21	0.45	0.064
C10–C14	σ	1.96855	C9–C10	σ^*	0.02110	15.29	1.22	0.060
C11–C12	σ	1.97260	C10–C11	σ^*	0.03420	18.93	1.26	0.068
C12–H12	σ	1.97720	C8–C13	σ^*	0.02300	14.67	1.07	0.055
C12–H12	σ	1.97720	C10–C11	σ^*	0.03420	17.84	1.08	0.061
C12–C13	σ	1.97210	O3–C8	σ^*	0.02948	13.50	1.07	0.052
C12–C13	σ	1.97210	O4–C11	σ^*	0.03285	15.34	1.06	0.056
C12–C13	π	1.71752	C8–C9	π^*	0.36558	80.67	0.28	0.067
C12–C13	π	1.71752	C10–C11	π^*	0.42279	75.53	0.31	0.069
C13–H13	σ	1.97744	C8–C9	σ^*	0.02751	17.93	1.09	0.061
C13–H13	σ	1.97744	C11–C12	σ^*	0.02153	13.91	1.06	0.053
C14–C15	σ	1.97636	C9–C10	σ^*	0.02110	13.33	1.29	0.057
C14–C15	π	1.80442	S1–C17	σ^*	0.02626	20.27	0.42	0.042

Table 4. (Continuation) Selected second-order perturbation energies $E^{(2)}$ associated with $i \rightarrow j$ delocalization in gas phase.

Donor orbital (i)	Type	ED/e	Acceptor orbital (j)	Type	ED/e	$E^{(2)}$ [kJ/mol] ^a	$E(j)-E(i)$ [a.u.] ^b	$F(i,j)$ [a.u.] ^c
C14–C15	π	1.80442	O5–C16	π^*	0.28744	91.54	0.30	0.074
C14–C15	π	1.80442	C10–C11	π^*	0.42279	43.76	0.32	0.055
C15–H15	σ	1.97420	O4–C16	σ^*	0.12395	17.72	0.84	0.055
C15–H15	σ	1.97420	C10–C14	σ^*	0.03343	19.52	1.23	0.068
C15–C16	σ	1.98160	C14–C15	σ^*	0.01954	12.54	1.32	0.056
C15–C16	σ	1.98160	C14–C17	σ^*	0.02814	14.33	1.56	0.066
C17–H17B	σ	1.97909	C10–C14	σ^*	0.03343	14.96	1.23	0.059
C19–C20	σ	1.97909	N6–C18	σ^*	0.05998	15.04	1.09	0.057
C21–C22	σ	1.98228	N6–C18	σ^*	0.05998	14.08	1.09	0.055
C21–C22	σ	1.98228	C10–C14	σ^*	0.03343	20.64	1.33	0.073
C21–C22	σ	1.98228	C14–C15	π^*	0.16017	25.53	0.81	0.065
C21–C22	σ	1.98228	C14–C17	σ^*	0.02814	41.00	1.49	0.108
C21–C22	σ	1.98228	C22–H22A	σ^*	0.02002	100.57	5.55	0.326
C22–H22A	σ	1.98004	C10–C14	σ^*	0.03343	18.93	1.22	0.067
C22–H22A	σ	1.98004	C14–C17	σ^*	0.02814	38.58	1.39	0.101
C22–H22A	σ	1.98004	C15–H15	σ^*	0.01325	14.79	1.12	0.056
C22–H22A	σ	1.98004	C21–H21A	σ^*	0.01457	21.69	0.94	0.063
C22–H22A	σ	1.98004	C21–C22	σ^*	0.01296	15.46	2.76	0.090
C22–H22A	σ	1.98004	C22–H22A	σ^*	0.02002	66.54	5.44	0.263
C22–H22A	σ	1.98004	C22–H22B	σ^*	0.02002	51.99	2.82	0.168
C22–H22B	σ	1.98156	C10–C14	σ^*	0.03343	61.61	1.21	0.120
C22–H22B	σ	1.98156	C14–C15	π^*	0.16017	52.54	0.70	0.087
C22–H22B	σ	1.98156	C14–C17	σ^*	0.02814	118.16	1.38	0.177
C22–H22B	σ	1.98156	C15–H15	σ^*	0.01325	46.94	1.11	0.100
C22–H22B	σ	1.98156	C22–H22A	σ^*	0.02002	269.02	5.44	0.528
C22–H22B	σ	1.98156	C22–H22B	σ^*	0.01560	33.27	2.82	0.134
S1	LP(1)	1.97272	S2–C18	π^*	0.02661	28.34	0.93	0.071
S1	LP(2)	1.81217	S2–C18	σ^*	0.50942	126.61	0.18	0.072
S2	LP(1)	1.97823	S1–C18	σ^*	0.11776	19.35	0.86	0.058
S2	LP(1)	1.97823	N6–C18	σ^*	0.05998	13.83	1.18	0.056
S2	LP(2)	1.82347	S1–C18	σ^*	0.11776	69.05	0.35	0.068
S2	LP(2)	1.82347	N6–C18	σ^*	0.05998	46.73	0.67	0.080
S2	LP(2)	1.82347	C17–H17B	σ^*	0.03283	16.63	0.61	0.046
O3	LP(1)	1.96313	C8–C9	σ^*	0.02751	29.05	1.11	0.079
O3	LP(2)	1.84590	C7–H7A	σ^*	0.01902	23.36	0.69	0.057
O3	LP(2)	1.84590	C7–H7C	σ^*	0.01908	23.53	0.69	0.058
O3	LP(2)	1.84590	C8–C9	π^*	0.36558	125.23	0.34	0.095
O4	LP(1)	1.96311	C10–C11	σ^*	0.03420	26.54	1.09	0.074
O4	LP(1)	1.96311	C15–C16	σ^*	0.05477	18.76	1.00	0.060
O4	LP(2)	1.74309	O5–C16	π^*	0.28744	146.13	0.35	0.100

Table 4. (Continuation) Selected second-order perturbation energies $E^{(2)}$ associated with $i \rightarrow j$ delocalization in gas phase.

Donor orbital (i)	Type	ED/e	Acceptor orbital (j)	Type	ED/e	$E^{(2)}$ [kJ/mol] ^a	$E(j)-E(i)$ [a.u.] ^b	$F(i,j)$ [a.u.] ^c
O4	LP(2)	1.74309	C10–C11	π^*	0.42279	113.65	0.37	0.094
O5	LP(2)	1.83314	O4–C16	σ^*	0.12395	156.33	0.57	0.131
O5	LP(2)	1.83314	C15–C16	σ^*	0.05477	66.75	0.70	0.097
N6	LP(1)	1.61189	S2–C18	σ^*	0.50942	357.01	0.19	0.118
N6	LP(1)	1.61189	C19–H19A	σ^*	0.02121	23.61	0.65	0.060
N6	LP(1)	1.61189	C19–H19B	σ^*	0.01621	13.54	0.67	0.046
O4–C16	σ^*	0.12395	O4–C11	σ^*	0.03285	114.19	0.02	0.080
O5–C16	π^*	0.28744	C14–C15	π^*	0.16017	31.39	0.17	0.067
C8–C9	π^*	0.36558	C10–C11	π^*	0.42279	532.95	0.02	0.077
C8–C9	π^*	0.36558	C12–C13	π^*	0.29806	830.56	0.01	0.082
C10–C11	π^*	0.42279	C14–C15	π^*	0.16017	135.68	0.14	0.113
C10–C11	π^*	0.42279	C14–C17	σ^*	0.02814	14.08	0.83	0.099
C10–C11	π^*	0.42279	C22–H22A	σ^*	0.02002	18.68	4.89	0.280
C14–C15	π^*	0.16017	C10–C14	σ^*	0.03343	24.28	0.52	0.158
C14–C15	π^*	0.16017	C14–C17	σ^*	0.02814	36.65	0.69	0.226
C14–C15	π^*	0.16017	C15–H15	σ^*	0.01325	14.42	0.41	0.114
C14–C15	π^*	0.16017	C22–H22A	σ^*	0.02002	60.61	4.74	0.780

^a $E^{(2)}$ energy of hyper conjugative interactions^bEnergy difference between donor and acceptor i and j NBO orbitals^c F_{ij} is the Fock matrix element between i and j NBO orbitals

The FMO plays an important role in the electric and optical properties, as well as in UV-Vis spectra and chemical reactions [71, 72]. Fig. 6 shows the distributions and energy levels of the HOMO-1, HOMO, LUMO and LUMO+1 orbitals calculated at the B3LYP/6-311++G(d,p) level for the title molecule. As can be seen from Fig. 6, both for the HOMO and HOMO-1, the electrons are delocalized on the sulfur atoms of the pyrrolidine-1-carbodithioate. For the LUMO and LUMO+1, the electrons are mainly delocalized on the 2-oxo-2H-chromen ring, C14–C17 bond and S1 atom. The value of the energy separation between the HOMO and LUMO is 1.42 eV. Considering the chemical hardness, small HOMO-LUMO gap (ΔE_{H-L}) means a soft molecule and large ΔE_{H-L} means a hard molecule. One can also relate the stability of the molecule to hardness, which means that the molecule with the least ΔE_{H-L} is more reactive and less stable [73]. The η and S can be calculated using the HOMO and LUMO energy values

for a molecule as follows: $\eta = (E_{LUMO} - E_{HOMO})/2$ and $S = 1/2\eta$ [60], where E_{LUMO} and E_{HOMO} are LUMO and HOMO energies, respectively. The calculated values of η and S for the title compound are 0.71 eV and 0.70 eV⁻¹, respectively.

3.8. Molecular electrostatic potential

Molecular electrostatic potential (MEP) mapping is very useful for understanding the sites for electrophilic attack and nucleophilic reactions as well as hydrogen bonding interactions [74]. Red-electron rich or partially negative charge regions of MEP are related to electrophilic reactivity and the blue-electron deficient or partially positive charge regions of MEP are related to nucleophilic reactivity shown in Fig. 7. The MEP clearly indicates that the electron rich centres were found around the O3, O5 and S2 atoms. The negative $V(r)$ values are -0.023 a.u. for O3 atom, -0.103 a.u. for O5 and -0.035 a.u. for S2 atom.

Table 5. Natural atomic charges (e) of (6-Methoxy-2-oxo-2H-chromen-4-yl)-methyl pyrrolidine-1-carbodithioate.

Atom	B3LYP	Atom	B3LYP	Atom	B3LYP
S1	0.24719	C10	-0.11967	C18	-0.05156
S2	-0.16350	C11	0.32460	C19	-0.17943
O3	-0.54097	C12	-0.19651	H19A	0.20289
O4	-0.51251	H12	0.22618	H19B	0.21295
O5	-0.56201	C13	-0.21046	C20	-0.38867
N6	-0.49501	H13	0.22257	H20A	0.19988
C7	-0.20596	C14	0.03099	H20B	0.21342
H7A	0.16955	C15	-0.28039	C21	-0.39439
H7B	0.19436	H15	0.23948	H21A	0.20043
H7C	0.16919	C16	0.75023	H21B	0.21463
C8	0.31283	C17	-0.53537	C22	-0.16780
C9	-0.25921	H17A	0.22481	H22A	0.20388
H9	0.21104	H17B	0.26817	H22B	0.22427

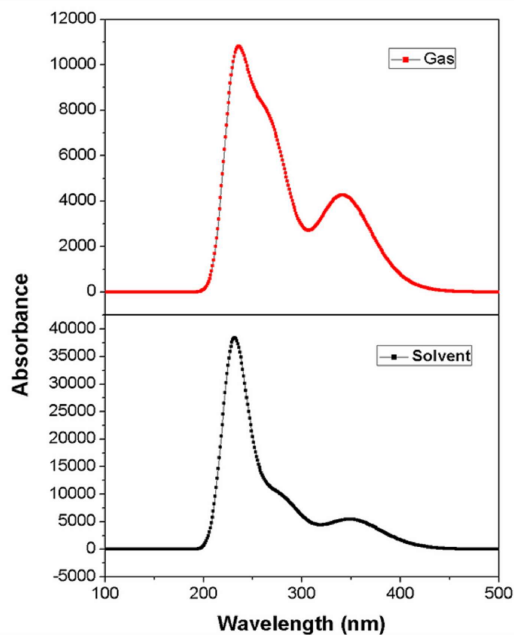


Fig. 5. Theoretical UV-Vis spectra of (6-Methoxy-2-oxo-2H-chromen-4-yl)-methyl pyrrolidine-1-carbodithioate. gas (top) and DMSO (bottom).

Thus, it could be predicted that an electrophile would preferentially attack the title molecule at O5 atom. On the other hand, a maximum positive region is localized on the methyl nearby with a value of +0.069 a.u. indicating a possible site for

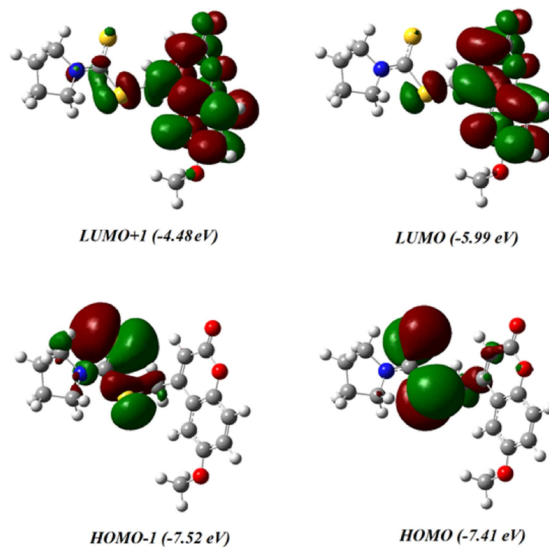


Fig. 6. Molecular orbital surfaces and energy levels of (6-Methoxy-2-oxo-2H-chromen-4-yl)-methyl pyrrolidine-1-carbodithioate.

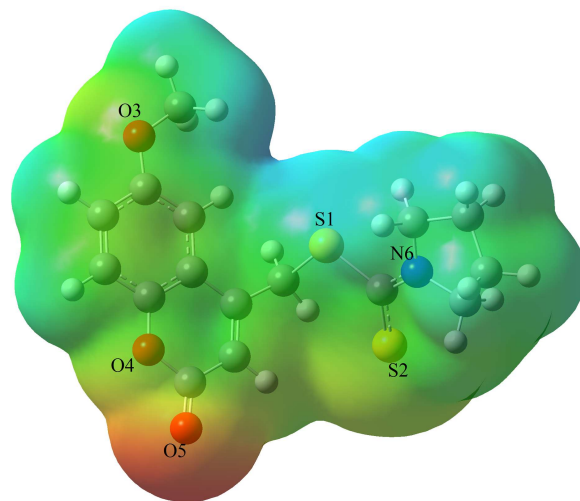


Fig. 7. The total electron density mapped with electrostatic potential of the title compound.

nucleophilic attack. So, the MEP surfaces clearly indicate that positive potential sites are around methylene and methyl hydrogen atoms. These sites give information that the compound can have metallic bonding and intermolecular interactions [73].

3.9. Non-linear optical properties

Nonlinear optics (NLO) is at the forefront of current research because of its importance in providing the key functions of frequency shifting, optical switching, optical modulation, optical logic, and optical memory for emerging technologies in areas such as telecommunications, signal processing, and optical interconnections [75, 76].

The dipole moment (μ), polarizability (α) and first hyperpolarizability (β) values of the title molecule were computed at the B3LYP/6-311++G(d,p) level using the Gaussian 09W program package. Calculations of the polar properties (α and β) from the Gaussian output have been explained in detail previously [77], and DFT has been used extensively as an effective method to investigate organic NLO materials [78, 79].

The calculated values of μ , α and β are 9.007 Debye, 38.299 Å³ and 4.868 esu for the title compound. Urea is used as one of the prototypical molecules in the study of NLO properties of molecular systems. Therefore, it has been used frequently as a threshold value for comparative purposes [78]. The values of α and β of the title compound are greater than those of urea (the α and β of urea are 5.042 Å³ and 0.78×10^{-30} esu obtained using the B3LYP/6-311++G(d,p) method) [22]. Theoretically, the β value of the title compound is of 6.24 times magnitude of urea. When we compare it with the similar compounds in the literature, the calculated value of β of the title compound is smaller than those of 9-methoxy-2H-furo[3,2-g]chromen-2-one ($\beta = 5.2983 \times 10^{-30}$ esu calculated with B3LYP/6-311++G(d,p) method) [80] and 6-phenylazo-3-(p-tolyl)-2H-chromen-2-one ($\beta = 34.528 \times 10^{-30}$ esu calculated with B3LYP/6-311++G(d,p) method) [81]. According to the magnitude of β , the title coumarin compound may be a potential applicant in the development of NLO materials.

3.10. Thermodynamic properties

The standard thermodynamic functions: entropy (S_m^0), heat capacity ($C_{p,m}^0$) and enthalpy

(H_m^0) were obtained on the basis of B3LYP/6-311++G(d,p) vibrational analysis and statistical thermodynamics and listed in Table 6. The Table shows that the S_m^0 , $C_{p,m}^0$ and H_m^0 increase at any temperature from 200.00 K to 600.00 K, because the intensities of the molecular vibration increase with the increasing temperature.

The correlations equations between these thermodynamic properties and temperatures T are as follows:

$$C_{p,m}^0 = -11.97047 + 1.36407T - 6.32498 \times 10^{-4}T^2$$

$$(R^2 = 0.99978) \quad (2)$$

$$S_m^0 = 290.75334 + 1.33432T - 2.92022 \times 10^{-5}T^2$$

$$(R^2 = 1) \quad (3)$$

$$H_m^0 = -6.01208 + 0.08769T + 4.33528 \times 10^{-4}T^2$$

$$(R^2 = 0.99995) \quad (4)$$

These equations will be helpful for the further studies of the title compound [82, 83].

Table 6. Thermodynamic properties at different temperatures at B3LYP/6-311++G(d,p) level.

T [K]	H_m^0 [kJ·mol ⁻¹]	$C_{p,m}^0$ [J·mol ⁻¹ ·K ⁻¹]	S_m^0 [J·mol ⁻¹ ·K ⁻¹]
200	29.30	237.84	545.94
250	42.84	287.79	606.22
300	58.89	338.28	664.70
350	77.45	387.27	721.80
400	98.39	433.17	777.68
450	121.55	475.18	832.15
500	146.67	513.09	885.07
550	173.63	547.07	936.40
600	202.18	577.55	986.06

4. Conclusions

In this study, we have calculated the geometric parameters, vibrational frequencies and chemical shifts of (6-Methoxy-2-oxo-2H-chromen-4-yl)-methyl pyrrolidine-1-carbodithioate using

the DFT/B3LYP and HF methods in conjunction with the 6-311++G(d,p) basis set. The comparisons between the calculated results and the X-ray experimental data show that HF method is better than B3LYP method in evaluating bond lengths. However, the B3LYP method seems to be more appropriate than HF method for predicting the bond angles and 3D geometry of the title compound. The vibrational frequencies are exactly assigned to its molecular structure with the aid of the theoretical calculations at B3LYP/6-311++G(d,p) and HF/6-311++G(d,p) levels, in which the experimental and theoretical results support each other. Furthermore, the calculated electronic absorption wavelengths and ^1H and ^{13}C NMR chemical shift values of the title compound in gas phase and solvent media can be built into the database for other chromen and pyrrolidine derivatives. It will be helpful for the design and synthesis of new materials. The stabilization energies were obtained from the second-order perturbation theory. The NBO analysis revealed that the $\pi^* \rightarrow \pi^*$ interactions give the strongest stabilization to the system. The correlations between the statistical thermodynamic properties (enthalpy, entropy, heat capacity) and temperature were also obtained. The calculated first order hyperpolarizability of the title compound was 6.24 times greater than that of urea.

References

- [1] LISGARTEN J.N., POTTER B.S., AYMAMI J., OKETCH-RABAH H., PALMER, R.A., *J. Chem. Crystallogr.*, 33 (2003), 149.
- [2] SHARMA P.N., SHOEB A., KAPIL R.S., POPLI S.P., *Indian J. Chem. B*, 17 (1979), 299.
- [3] SHARMA P.N., SHOEB A., KAPIL R.S., POPLI S.P., *Indian J. Chem. B*, 19 (1980), 938.
- [4] SHARMA P.N., SHOEB A., KAPIL R.S., POPLI S.P., *Phytochemistry*, 20 (1981), 335.
- [5] Enraf-Nonius CAD-4 Express '88 Software, Enraf-Nonius: Delft, Holland, 1988.
- [6] NORTH A.C.T., PHILIPS D.C., MATHEWS F.S., *Acta Crystallogr. A*, 24 (1968), 351.
- [7] JONES G., JACKSON W.R., CHOI C., BERGMARK W.R., *J. Phys. Chem.*, 89 (1985), 294.
- [8] TRENOR S.R., SHULTZ A.R., LOVE B.J., LONG T.E., *Chem. Rev.*, 104 (2004), 3059.
- [9] HUNG T.T., LU Y.J., LIAO W.Y., HUANG C.L., *IEEE T. Magn.*, 43 (2007), 867.
- [10] KUMAR K.M., KOUR D., KAPOOR K., MAHA-BALESHWARAIAH N.M., KOTRESH O., GUPTA V.K., KANT R., *Acta Crystallogr. E*, 68 (2012), o878.
- [11] HAULT J.R.S., PAYA M., *Vascul. Pharmacol.*, 27 (1996), 713.
- [12] RIVEIRO M.E., KIMPE N.D., MOGLIONI A., VAZQUEZ R., MONCZOR F., SHAYO C., DAVIO C., *Curr. Med. Chem.*, 17 (2010), 1325.
- [13] SIVAGURU P., SANDHIYA R., ADHIYAMAN M., LALITHA A., *Tetrahedron Lett.*, 57 (23) (2016), 2496.
- [14] ZHANG Y., GUO Z.J., YOU X.Z., *J. Am. Chem. Soc.*, 123 (2001), 9378.
- [15] PROFT DE F., GEERLINGS P., *Chem. Rev.*, 101 (2001), 1451.
- [16] BINGÖL ALPASLAN Y., GÖKCE H., ALPASLAN G., MACIT M., *J. Mol. Struct.*, 1097 (2015), 171.
- [17] TANAK H., ERŞAHİN F., KÖYSAL Y., AĞAR E., IŞIK Ş., YAVUZ M., *J. Mol. Model.*, 15 (2009), 1281.
- [18] MAHABALESHWARAIAH N.M., KUMAR K.M., KOTRESH O., AL-ERYANI W.F.A., DEVARAJEGOWDA H.C., *Acta Crystallogr. E*, 68 (2012), o1566.
- [19] FRISCH M.J., TRUCKS G.W., SCHLEGEL H.B., *Gaussian 09, Revision C.01*, Gaussian, Inc.: Wallingford, CT, 2009.
- [20] DENNINGTON R., KEITH T., MILLAM J., *GaussView, Version 5*, Semichem Inc.: Shawnee Mission, KS, 2009.
- [21] WOLINSKI K., HINTON J.F., PULAY P., *J. Am. Chem. Soc.*, 112 (1990), 8251.
- [22] TOY M., TANAK H., *Spectrochim. Acta A*, 152 (2016), 530.
- [23] CANCČS E., MENNUCCI B., TOMASI J., *J. Chem. Phys.*, 107 (1997), 3032.
- [24] PHAKHODEE W., LAPHOOKHIEO S., PRIOR T.J., RUJIWATRA A., *Acta Crystallogr. E*, 68 (2012), o3421.
- [25] DEVARAJEGOWDA H.C., KUMAR K.M., SEENIVASA S., ARUNKASHI H.K., KOTRESH O., *Acta Crystallogr. E*, 69 (2013), o192.
- [26] SINHA S., OSMAN H., WAHAB H.A., HEMAMALINI M., FUN H.K., *Acta Crystallogr. E*, 67 (2011), o3457.
- [27] TANAK H., AGAR A.A., BÜYÜKGÜNGÖR O., *Spectrochim. Acta A*, 87 (2012), 15.
- [28] AGAR A.A., TANAK H., YAVUZ M., *Mol. Phys.*, 108 (2010), 1759.
- [29] TEIMOURI A., EMAMI M., CHERMAHINI A.N., DABAGH H.A., *Spectrochim. Acta A*, 71 (2009), 1749.
- [30] DERELI Ö., BAHÇELI S., ABBAS A., NASEER M.M., *Monatsh. Chem.*, 146 (2015), 1473.
- [31] SILVERSTEIN R.M., BASSELER G.C., MORILL C., *Spectroscopic Identification of Organic Compounds*, Wiley, New York, 1981.
- [32] RAHMAN T.U., ARFAN M., MAHMOOD T., LI-AQAT W., GILANI M.A., UDDI G., LUDWIG R., ZAMAN K., CHOUDHARY M.I., KHATTAK K.F., AYUB K., *Spectrochim. Acta A*, 146 (2015), 24.
- [33] SINGH R.N., PRASAD S.C., *Spectrochim. Acta A*, 34 (1974), 39.

- [34] SARIKAYA K.E., DERELI Ö., *J. Mol. Struct.*, 1052 (2013), 214.
- [35] BABU P.C., SUNDARAGANESAN N., DERELI O., TURKKAN E., *Spectrochim. Acta A*, 79 (2011), 562.
- [36] SUBRAMANIAN N., SUNDARAGANESAN N., DERELI O., TURKKAN E., *Spectrochim. Acta A*, 83 (2011), 165.
- [37] KALAICHELVAN S., SUNDARAGANESAN N., DERELI O., SAYIN U., *Spectrochim. Acta A*, 85 (2012), 189.
- [38] LITVINOV G., *Proceedings of the XIII International Conference on Raman Spectroscopy*, Wurzburg, Germany, 1992.
- [39] EL-GOGARY T.M., SOLIMAN M.S., *Spectrochim. Acta A*, 57 (2001), 2647.
- [40] AL-SAADY A.A., LAANE J., *J. Mol. Struct.*, 830 (2007), 46.
- [41] PARLAK C., *J. Mol. Struct.*, 966 (2010), 1.
- [42] SUNDARAGANESAN N., ANAND B., MEGANATHAN C., DOMINIC JOSHUA B., SALEEM H., *Spectrochim. Acta A*, 69 (2008), 198.
- [43] ARJUNAN V., SANTHANAM R., SAKILADEVI S., MARCHEWKA M.K., MOHAN S., *J. Mol. Struct.*, 1037 (2013), 305.
- [44] MOGHADDAM F.M., FOROUSHANI B.K., *J. Mol. Struct.*, 1065 (2014), 235.
- [45] SAJAN D., ERDOGDU Y., RESHMY R., DERELI Ö., KURIEN THOMAS K., HUBERT JOE I., *Spectrochim. Acta A*, 82 (2011), 118.
- [46] SRI N.U., CHAITANYA K., PRASAD M.V.S., VEERAI AH V., VEERAI AH A., *Spectrochim. Acta A*, 97 (2012), 728.
- [47] PRABHUA T., PERIANDY S., RAMALINGAM S., *Spectrochim. Acta A*, 83 (2011), 8.
- [48] TECKLENBURG M.M.J., KOSNAK D.J., BHATNAGAR A., MOHANTY D.K., *J. Raman Spectrosc.*, 28 (1997), 755.
- [49] PAJAZK J., ROSPENK M., RAMAEKERS R., MAES G., GŁOWIAK T., SOBCZYK L., *Chem. Phys.*, 278 (2002), 89.
- [50] ARIVAZHAGAN M., KRISHNAKUMAR V., JOHN-AVIER R., ILANGO V., BALACHANDRAN K., *Spectrochim. Acta A*, 72 (2009), 941.
- [51] RAHMAN T.U., ARFAN M., MAHMOOD T., LI-AQAT W., GILANI M.A., UDDIN G., LUDWING R., ZAMAN K., CHOUDHARY M.I., KHATTAK K.F., AYUB K., *Spectrochim. Acta A*, 146 (2015), 24.
- [52] SILVERSTEIN R.M., WEBSTOR F.X., *Spectrometric Identification of Organic Compounds*, 6th ed., John Wiley & Sons, New York, 1998.
- [53] BELLAMY L.J., *The Infrared Spectra of Complex Molecules*, Chapman and Hall, London, 1975.
- [54] RAO C.N., *Chemical Application of Infrared Spectroscopy*, Academic Press, New York, 1963.
- [55] THANIKACHALAM V., PERIYANAYAGASAMY V., JAYABHARATHI J., MANIKANDAN G., SALEEM H., SUBASHCHANDRABOSE S., ERDOGDU Y., *Spectrochim. Acta A*, 87 (2012), 86.
- [56] MANI P., UMAMAHESWARI H., DOMINIC JOSHUA B., SUNDARAGANESAN N., *J. Mol. Struct.*, 868 (2008), 44.
- [57] KAKKAR R., DUA A., ZAIDI S., *Spectrochim. Acta A*, 68 (2007), 1362.
- [58] TANAK H., *J. Mol. Struct.*, 1090 (2015), 86.
- [59] TANAK H., AGAR A.A., BÜYÜKGÜNGÖR O., *Spectrochim. Acta A*, 118 (2014), 672.
- [60] RAJESH P., GUNASEKARAN S., GNANASAMBANDAN T., SESHADRI S., *Spectrochim. Acta A*, 137 (2015), 1184.
- [61] RAMYA T., GUNASEKARAN S., RAMKUMAAR G.R., *Spectrochim. Acta A*, 149 (2015), 132.
- [62] KRISHNAN G.K., SIVAKUMAR R., THANIKACHALAM V., SALEEM H., AROCKIA DOSS M., *Spectrochim. Acta A*, 144 (2015), 29.
- [63] ERDOGDU Y., SAGLAM S., DERELI Ö., *Opt. Spectrosc.*, 119 (2015), 441.
- [64] RAMYA T., GUNASEKARAN S., RAMKUMAAR G.R., *Spectrochim. Acta A*, 149 (2015), 132.
- [65] PISANI L., CATTO M., NICOLOTTI O., GROSSI G., BRACCIO DI M., SOTO-OTERO R., MENDEZ-ALVAREZ E., STEFANACHI A., GADALETA D., CAROTTI A., *Eur. J. Med. Chem.*, 70 (2013), 723.
- [66] JAMES C., AMAL RAJ A., REGHUNATHAN R., HUBERT JOE I., JAYAKUMAR V.S., *J. Raman Spectrosc.*, 37 (2006), 1381.
- [67] LIU J.N., CHEN Z.R., YUAN S.F., ZHEJIANG J., *J. Zhejiang Univ.-Sc. B*, 6 (2005), 584.
- [68] MUTHU S., PRASATH M., *Spectrochim. Acta A*, 115 (2013), 789.
- [69] SCHWENKE D.W., TRUHLAR D.G., *J. Chem. Phys.*, 82 (1985), 2418.
- [70] GUTOWSKI M., CHALASINSKI G., *J. Chem. Phys.*, 98 (1993), 4728.
- [71] TANAK H., PAWLUS K., MARCHEWKA M.K., PIETRASZKO A., *Spectrochim. Acta A*, 118 (2014), 82.
- [72] FLEMING I., *Frontier Orbitals and Organic Chemical Reactions*, Wiley, London, 1976.
- [73] EVECEN M., TANAK H., TINMAZ F., DEGE N., İLHAN İ.Ö., *J. Mol. Struct.*, 1126 (2016), 117.
- [74] SINGH S.J., PANDEY S.M., *Indian J. Pure Ap. Phys.*, 12 (1974), 300.
- [75] TANAK H., *J. Phys. Chem. A*, 115 (2011), 13865.
- [76] SAJAN D., JOE H., JAYAKUMAR V.S., ZALESKI J., *J. Mol. Struct.*, 785 (2006), 43.
- [77] THANTHIRIWATTE K.S., SILVA DE N.K.M., *J. Mol. Struct.-Theochem*, 617 (2002), 169.
- [78] SUN Y.X., HAO Q.L., WEI W.X., YU Z.X., LU L.D., WANG X., WANG Y.S., *J. Mol. Struct.*, 929 (2009), 10.
- [79] TANAK H., *Int. J. Quantum Chem.*, 112 (2012), 2392.

- [80] SWARNALATHA N., GUNASEKARAN S., MUTHU S., NAGARAJAN M., *Spectrochim. Acta A*, 137 (2015), 721.
- [81] MANIMEKALAI A., VIJAYALAKSHMI N., *Spectrochim. Acta A*, 136 (2015), 388.
- [82] ZHAO P.S., XU J.M., ZHANG W.G., JIAN F.F., ZHANG L., *Struct. Chem.*, 18 (2007), 993.
- [83] TANAK H., *Mol. Phys.*, 112 (2014), 1553.

Received 2016-05-05

Accepted 2016-10-09